Int. J. Solids Structures Vol. 23, No. 11, pp. 1521–1534, 1987
Printed in Great Britain.

0020-7683/87 $3.00 + .00
© 1987 Pergamon Journals Ltd.

A CONSTITUTIVE THEORY FOR PROGRESSIVELY DETERIORATING BRITTLE SOLIDS

R. ILANKAMBAN† and D. KRAJCINOVIC
Department of Civil Engineering, Mechanics and Metallurgy, University of Illinois at Chicago, Chicago, IL 60680, U.S.A.

(*Received April* 1985; *in revised form May* 1986)

Abstract—Assuming that micro-fracturing is the dominant mode of irreversible micro-structural change, the internal degradation of a brittle material is described by a set of internal variables that reflect the microcrack density and distribution. The kinetic equation for the crack evolution is written assuming the existence of a flow potential (damage surface). Predictions of the theory are compared with the microscopic and macroscopic experimental observations on rock. Also, it is shown that for a fixed crack distribution the symmetry of the stiffness tensor varies with the applied stress.

1. INTRODUCTION

In general, deformation of a solid is accompanied by micro-structural rearrangements in the form of crystalline slip, twinning, diffusion and microcracking. These changes in the microstructure alter the thermo-mechanical properties (stiffness, thermal conductivity, etc.) of the solid. Macroscopically, these changes are manifested by the nonlinearity and irreversibility of the response. This study is based on the premise that the predictive ability of a constitutive theory will, in general, be proportional to the degree to which it models the underlying microstructure and its kinetics. In this paper, phenomenological constitutive equations for the mechanical response of a solid progressively weakened by an arbitrary distribution of microcracks are presented. The microcracks are assumed to be plane and flat and of characteristic dimension small enough to allow for a representation by continuum variables.

The loading process is assumed to be isothermal and quasi-static, and the material rate insensitive. The proposed formulation can be applied to the prediction of the pre-failure response of brittle solids such as rocks and concrete under multi-axial and non-proportional loading conditions.

2. INTERNAL VARIABLES

It is important that not only the internal variables are uniquely defined by the micro-structural arrangement, but also a given set of the internal variables should define a macroscopically unique state. This cannot be easily achieved if the values of the internal variables are defined to be stress dependent. For example, in an elastic solid, cracks subjected to pure compression across their normal cause no discontinuity in the displacement field or reduction in the stiffness. Consequently, a variable defined as a function of change in the stiffness or of displacement discontinuity due to cracks cannot differentiate a solid with cracks under compression from the one without cracks.

In the present formulation, we employ a continuum internal variable representation of microcracks proposed by Krajcinovic (1985), which meets the above uniqueness condition and has a direct physical meaning. Consider a continuum point in a solid permeated by numerous plane flat microcracks. Since a continuum point is endowed with the average properties of the surrounding material of finite volume, in general, it is possible that microcracks of different orientations be simultaneously present at a point. Hence, a function $\omega(\mathbf{N})$ of orientation (where $\mathbf{N}$ is a crack orientation vector which varies over a unit sphere of orientations and $\omega(\mathbf{N})$ is some volume average of the area of the cracks with the normal

† Present address: Engineering Technology Associates, 1895 Crooks Road, Troy, MI 48084, U.S.A.

N) can be defined as the internal state variable that describes the microcrack distribution. Since orientation of a crack can be taken either as N or as $-\mathbf{N}$, it follows that $\omega(\mathbf{N}) = \omega(-\mathbf{N})$. To facilitate the computations, instead of the continuous function of orientation $\omega(\mathbf{N})$, the values of that function, $\omega^1, \omega^2, \ldots, \omega^n$, at a finite number (say n) of *a priori* selected orientations, $\mathbf{N}^1, \mathbf{N}^2, \ldots, \mathbf{N}^n$, are taken as the internal state variables. These orientation vectors are taken to be uniformly distributed over a unit hemisphere of orientations which is fixed in the material coordinate system. The questions of scale and of averaging of microcrack distribution into continuum variables are discussed in Krajcinovic (1985).

3. GOVERNING EQUATIONS

Assuming small deformation and restricting the discussion to a homogeneous temperature distribution and isothermal processes, the state of the material is defined by the strain tensor $\boldsymbol{\varepsilon}$ and the set of internal variables $[(\omega^i, N^i),\ i = 1, \ldots, n]$ which describe the microcrack distribution. The response functions of interest, stress $\boldsymbol{\sigma}$ and the Helmholtz free energy ψ, are, therefore, of the following form:

$$\begin{aligned} \boldsymbol{\sigma} &= \hat{\boldsymbol{\sigma}}[\boldsymbol{\varepsilon}; (\omega^i, \mathbf{N}^i), i = 1, \ldots, n] \\ \psi &= \hat{\psi}[\boldsymbol{\varepsilon}; (\omega^i, \mathbf{N}^i), i = 1, \ldots, n]. \end{aligned} \tag{1}$$

The forms of the above response functions are not independent since they must satisfy the Clausius–Duhem inequality, which for the present purpose can be written as follows:

$$\sigma_{IJ}\delta\varepsilon_{IJ} - \rho\delta\psi \geqslant 0 \tag{2}$$

where ρ is the mass density while δ denotes increment.

Substituting eqns (1) in inequality (2), it follows that

$$\left(\sigma_{IJ} - \rho\frac{\partial\psi}{\partial\varepsilon_{IJ}}\right)\partial\varepsilon_{IJ} - \sum_i \rho\left(\frac{\partial\psi}{\partial\omega^i}\right)\delta\omega^i \geqslant 0. \tag{3}$$

Following the arguments of Coleman and Gurtin (1967), we assume that the strain $\boldsymbol{\varepsilon}$ can be varied independent of $\delta\omega^i$. Thus inequality (3) is satisfied for arbitrary $\delta\boldsymbol{\varepsilon}$, if

$$\sigma_{IJ} = \rho\frac{\partial\psi}{\partial\varepsilon_{IJ}} \tag{4}$$

and

$$\sum_i R^i\delta\omega^i \geqslant 0 \tag{5}$$

where

$$R^i = -\rho\frac{\partial\psi}{\partial\omega^i} \tag{6}$$

is the thermodynamic force conjugate to ω^i.

The reduced form of the Clausius–Duhem inequality (5) implies that energy dissipation associated with any change in the microcrack distribution is always non-negative. Since using eqn (4) stress $\boldsymbol{\sigma}$ can be computed from ψ, the formulation will be complete providing that the specific constitutive assumptions can be made for the form of the Helmholtz free energy and for the evolution of the internal variables.

4. APPLICATION TO ROCK

Scanning electron microscope observations (Sprunt and Brace, 1974; Tapponnier and Brace, 1976; Wong, 1982) of specimens of rock stressed below peak stress show that the microcracking is the predominant stress induced change in the microstructure of the rock. Numerous cracks are observed in a volume of few grains. Consequently, preceding the stress failure the size and the number of microcracks would admit a continuum representation, and the present formulation would be valid in that range. In general, beyond the peak stress the microcracks coalesce to form macrocracks which henceforth dominate the response of the material.

4.1. *Helmholtz free energy (HFE)*

Virgin rock is assumed to be initially isotropic; and since the strain at the peak stress is typically of the order of 1%, the change in the mass density is neglected. Though a small hysteresis is observed in unloading and reloading, to focus on the main aspect of the theory, it is postulated that the response is linear in the absence of a change in the density and distribution of microcracks. Hence, as stress is a first-order derivative of HFE with respect to strain (see eqn (4)), the HFE must be second order in strain.

To arrive at a particular form of HFE, it is necessary to consider both microscopic and macroscopic experimental observations (Wawersik and Brace, 1971). In a brittle specimen subjected to uniaxial compression, microcracks first form on the planes that are nearly parallel to the axis of compression (AOC). Upon further loading, cracks form on the planes adjacent to above planes and on the planes inclined at about 45° to the AOC. The crack density has a global maximum on the planes parallel to the AOC, which are planes of maximum tensile strain but zero tensile stress; and a local maximum on the planes inclined at 45° to AOC, which are planes of maximum shear strain. Further, it is noticed that cracks parallel to the AOC contribute to the reduction in the axial stiffness and induce volumetric dilatancy. Since no tensile stress is applied across the planes parallel to the AOC, the prediction of the formation and the growth of microcracks in these planes and of their influence on the axial stiffness employing linear fracture theories are not obvious. Actually, the cracks in planes parallel to the AOC are associated either with the fluctuations of stresses about their expected value (Costin, 1983) or with kinking of the original mode II cracks (Nemat-Nasser and Horii, 1982). However, from a phenomenological point of view, it is assumed that the energy associated with a crack is related to tensile strain and shear strain rather than tensile stress and shear stress. The HFE can therefore be written using the isotropic invariants of $\boldsymbol{\varepsilon}$ and $[(\omega^i, \mathbf{N}^i), i = 1, \ldots, n]$ (Spencer, 1971)

$$\rho\psi = (\lambda/2)\varepsilon_{KK}\varepsilon_{LL} + \mu\varepsilon_{KL}\varepsilon_{KL} + C_1 \sum_i \omega^i [\langle N^i_K \varepsilon_{KL} N^i_L \rangle \langle N^i_M \varepsilon_{MN} N^i_N \rangle] + C_2 \sum_i \omega^i [N^i_K \varepsilon_{KL} \varepsilon_{LM} N^i_M - (N^i_K \varepsilon_{KL} N^i_L)(N^i_M \varepsilon_{MN} N^i_N)] \quad (7)$$

where λ, μ are Lame's constants, C_1, C_2 the material parameters associated with cracks, and $\langle\ \rangle$ Macaulay's bracket defined as

$$\langle x \rangle = \begin{cases} 1, & \text{if } x > 0 \\ 0, & \text{otherwise.} \end{cases}$$

Since $\mathbf{N}^i$ is a unit vector, the quantities within the first and second square brackets in eqn (7) are squares of the normal (tensile) and shear strain on the plane with the normal $\mathbf{N}^i$, respectively. Energy associated to the compressive strain over the faces of the cracks is taken to be zero. Despite the fact that the cracks impose a one-sided constraint on the displacement discontinuity, the stress–strain relation should be continuous. Differentiating with respect to $\boldsymbol{\varepsilon}$, one can verify that the proposed form of ψ is indeed C^1 continuous.

Lame's coefficients, λ and μ, are taken to be constant such that the first two terms on the right-hand side of eqn (7) correspond to the response of the solid in its virgin state. As

the energy storing capacity of a solid is diminished by the presence of cracks, the sum of the last two terms in eqn (7) should be non-positive. Since normal strain and shear strain on a crack can be varied independently, each of the above two terms in eqn (7) should be non-positive by itself. Moreover, since the crack density ω^i is non-negative and the terms within the brackets are the squares of the normal and shear strain, it follows that the material parameters C_1 and C_2 should be non-positive.

Substituting eqn (7) in eqn (4) we obtain

$$\sigma_{IJ} = \rho \frac{\partial \psi}{\partial \varepsilon_{IJ}} = K_{IJKL}\varepsilon_{KL} \tag{8}$$

where **K** is the stiffness tensor given by

$$K_{IJKL} = \lambda\delta_{IJ}\delta_{KL} + \mu(\delta_{IK}\delta_{JL} + \delta_{IL}\delta_{JK}) + 2C_1 \sum_i \omega^i H(i) N^i_I N^i_J N^i_K N^i_L$$
$$+ C_2/2 \sum_i \omega^i (\delta_{JK} N^i_I N^i_L + \delta_{JL} N^i_I N^i_K + \delta_{IL} N^i_J N^i_K + \delta_{IK} N^i_J N^i_L - 4 N^i_I N^i_J N^i_K N^i_L) \tag{9}$$

$$H(i) = \begin{cases} 1, & \text{if } N^i_K \varepsilon_{KL} N^i_L > 0 \\ 0, & \text{otherwise.} \end{cases}$$

The stiffness tensor **K** has the following symmetries:

$$K_{IJKL} = K_{KLIJ} = K_{JIKL} = K_{IJLK}. \tag{10}$$

Since in the third term on the right-hand side of eqn (9) the contribution of cracks under compression vanishes, the load induced anisotropy is reflected in eqn (9). For example, consider an isotropic distribution of microcracks, i.e. $\omega^1 = \omega^2 = \cdots = \omega^n = \omega$. Under hydrostatic tension all the cracks will experience tensile strain. In this case, from eqn (9), the stiffness tensor will be isotropic and takes the following form:

$$K_{IJKL} = \left[\lambda + \frac{4\pi}{15}\omega(C_1 - C_2)\right]\delta_{IJ}\delta_{KL} + \left[\mu + \frac{4\pi}{15}\omega(C_1 + 1.5C_2)\right](\delta_{IK}\delta_{JL} + \delta_{IL}\delta_{JK}).$$

However, in uniaxial compression along the X_1-axis, the cracks the plane normals of which subtend an angle less than $\sin^{-1}[1+\nu]^{-1/2}$ with the X_1-axis will experience compressive strain (here ν is the apparent Poisson's ratio). In this case the stiffness tensor ceases to be isotropic and becomes transversely isotropic, and is expressed as

$$K_{IJKL} = \lambda\delta_{IJ}\delta_{KL} + \left[\mu + \frac{\pi}{3}\omega C_2 a(3 - a^2)\right](\delta_{IK}\delta_{JL} + \delta_{IL}\delta_{JK}) + C_0\hat{K}_{IJKL}$$

where

$$\hat{K}_{1111} = \frac{2}{5}a^5; \quad \hat{K}_{2222} = \hat{K}_{3333} = \frac{3}{4}\left(a - \frac{2}{3}a^3 + \frac{a^5}{5}\right)$$

$$\hat{K}_{1122} = \hat{K}_{1212} = \hat{K}_{1133} = \hat{K}_{1313} = \frac{2}{3}a^3 - \frac{a^5}{5}$$

$$\hat{K}_{2233} = \hat{K}_{2323} = \frac{1}{3}\hat{K}_{2222}; \quad a = \left(\frac{\nu}{1+\nu}\right)^{5/2}; \quad C_0 = \pi(C_1 - C_2).$$

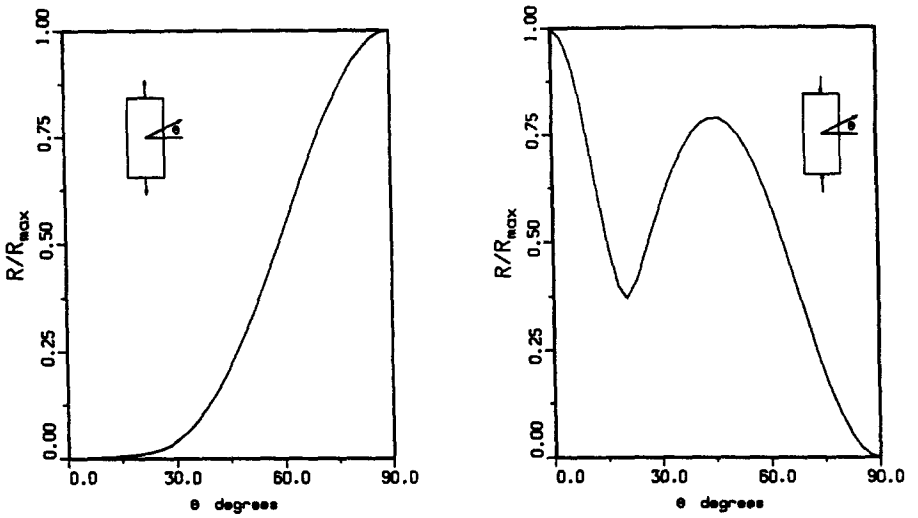

Fig. 1. Typical variation of the conjugate thermodynamic force R with orientation θ.

The remaining non-zero terms in $\hat{\mathbf{K}}$ are obtained from the symmetry conditions as in eqn (10).

From eqns (6) and (7), the conjugate thermodynamic force can be written as

$$R^i = -C_1\langle N^i_K\varepsilon_{KL}N^i_L\rangle\langle N^i_M\varepsilon_{MN}N^i_N\rangle - C_2[N^i_K\varepsilon_{KL}\varepsilon_{LM}N^i_M - (N^i_K\varepsilon_{KL}N^i_L)(N^i_M\varepsilon_{MN}N^i_N)]. \tag{11}$$

Since under uniaxial loading of an unconfined rock specimen the maximum microcrack density occurs in the planes perpendicular to the maximum tensile strain, the conjugate thermodynamic force must also have a maximum at these planes. This places the following restriction on the material parameters (Ilankamban, 1985):

$$2C_1 < C_2(1+\nu_m)/\nu_m < 0$$

where ν_m is the minimum apparent Poisson's ratio in uniaxial compression. Typical variation of the thermodynamic force of microcracking as a function of orientation, under uniaxial compression and tension, is shown in Fig. 1. From eqn (8), the stress increment can be written as

$$\delta\sigma_{IJ} = K_{IJKL}\,\delta\varepsilon_{KL} + \sum_i A^i_{IJ}\,\delta\omega^i \tag{12}$$

where

$$\begin{aligned} A^i_{IJ} &= \frac{\partial}{\partial\omega^i}\left(\rho\frac{\partial\psi}{\partial\varepsilon_{IJ}}\right) \approx \frac{\partial}{\partial\varepsilon_{IJ}}\left(\rho\frac{\partial\psi}{\partial\omega^i}\right) = -\frac{\partial R^i}{\partial\varepsilon_{IJ}} \\ &= -2C_1\langle N^i_K\varepsilon_{KL}N^i_L\rangle N^i_I N^i_J \\ &\quad - C_2[N^i_K\varepsilon_{KI}N^i_J + N^i_K\varepsilon_{KJ}N^i_I - 2(N^i_K\varepsilon_{KL}N^i_L)N^i_I N^i_J]. \end{aligned} \tag{13}$$

4.2. *Kinetics of crack growth*

Acoustic emission experiments on geo-materials (Holcomb, 1984) clearly show that there exists a finite region in strain (stress) space within which only elastic change occurs. The additional microcracking occurs only when loaded beyond that elastic region. Based on these observations, the following assumptions can be made:

(1) There exists a surface $g = 0$, in the strain space, which separates the elastic domain ($\delta\omega^i \equiv 0$ for all i) from the inelastic domain. It is further assumed that g depends on the strain ε only through the thermodynamic force conjugate to ω^i, i.e.

$$g = g[(\omega^i, R^i, \mathbf{N}^i), \quad i = 1, \ldots, n]. \tag{14}$$

Since R^i is an energy release rate, eqn (14) is an energy criterion for crack growth. The equation $g = 0$ represents the "damage surface" in the n-dimensional space of thermodynamic forces, enveloping the locus of all states which can be reached without dissipating energy.

(2) The crack growth is stable in the following sense

$$\sum_i \int_{S_1}^{S_2} (R^i - R_1^i)\, \mathrm{d}\omega^i \geqslant 0 \tag{15}$$

where S_1 is an initial state, S_2 any state achievable from S_1, and R_1^i the conjugate force at state S_1.

It can be noted that condition (15) is similar to Drucker's stability condition (Drucker, 1959) for a rigid plastic material. Following the arguments of the theory of plasticity, and identifying R^i with stress and ω^i with strain, it can be concluded that g is convex and the increments of ω^i are normal to the surface $g = 0$, i.e.

$$\delta\omega^i = k \frac{\partial g}{\partial R^i} \tag{16}$$

$$k = c \frac{\sum_m \left(\dfrac{\partial g}{\partial R^m} \delta R^m \right)}{\sum_j \left(-\dfrac{\partial g}{\partial \omega^j} \right) \left(\dfrac{\partial g}{\partial R^j} \right)}$$

$$c = \begin{cases} 1, & \text{if } g = 0 \text{ and } \sum_m \left(\dfrac{\partial g}{\partial R^m} \delta R^m \right) \geqslant 0 \\ 0, & \text{otherwise.} \end{cases}$$

It is assumed that further growth of cracks in a plane with the orientation $\mathbf{N}^j$ is possible when

$$g^j = R^j - \mathscr{R}^j[(\omega^i, \mathbf{N}^i), \quad i = 1, \ldots, n] = 0 \tag{17}$$

where $\mathscr{R}^j$ is a threshold parameter dependent on the state of microcracking. The form of $\mathscr{R}^j$ in eqn (17) defines the rate of crack growth with respect to loading and the degree of interaction between microcracks at different orientations. This can be compared with slips on the crystallographic plane, where slip on one plane affects (typically increases) the slip resistance of the adjacent planes (Hutchinson, 1976). However, in the absence of any experimental guidance, here it is assumed that the interaction is negligible. Thus from eqn (17)

$$g^j = R^j - \mathscr{R}^j(\omega^j) = 0. \tag{18}$$

Geometrically, constraints (18) (written for all $j = 1, \ldots, n$) define a polyhedral surface

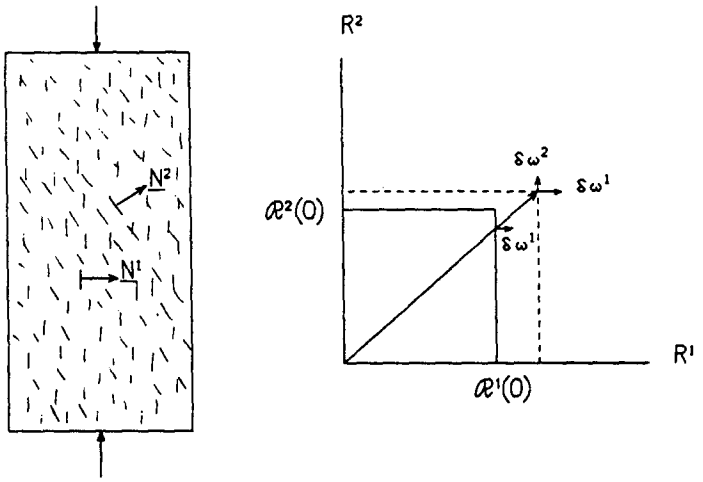

Fig. 2. The damage surface in the conjugate thermodynamic force space.

consisting of hyper-planes, which is illustrated for $n = 2$ in Fig. 2. For an initially isotropic material, the form of $\mathscr{R}^j$ will be identical for all $j = 1, \ldots, n$. In view of the strongly non-linear character of the process, a reasonable form of eqn (18) is

$$g^j = (R^j/\lambda)^p - (\mathscr{R}_0 + \omega^j) = 0 \tag{19}$$

where p and $\mathscr{R}_0$ are material parameters and λ is Lame's coefficient introduced as a non-dimensionalizing factor. The constant $\mathscr{R}_0$ defines the onset of microcracking in a plane.

From eqns (16) and (19), the increment in the crack density is

$$\delta\omega^i = c^i (p/\lambda)\,(R^i/\lambda)^{p-1}\,\delta R^i \tag{20}$$

where c^i is the loading index defined as

$$c^i = \begin{cases} 1, & \text{if } g^i = 0 \text{ and } (\partial g^i/\partial R^i)\,\delta R^i \geqslant 0 \\ 0, & \text{otherwise.} \end{cases} \tag{21}$$

From eqns (20) and (11), the increment in the crack density can be written in terms of the increment in strain as

$$\delta\omega^i = H^i_{KL}\,\delta\varepsilon_{KL} \tag{22}$$

where

$$H^i_{KL} = -c^i (p/\lambda)\,(R^i/\lambda)^{p-1} A^i_{KL}.$$

Substituting eqn (22) in eqn (12), the incremental stress–strain relation is obtained as

$$\delta\sigma_{IJ} = [K_{IJKL} + \bar{K}_{IJKL}]\,\delta\varepsilon_{KL} \tag{23}$$

where

$$\bar{K}_{IJKL} = \sum_i A^i_{IJ} H^i_{KL}.$$

During loading, both terms on the right-hand side of eqn (23) contain non-zero terms. During unloading, only the first term contributes to the stiffness. However, the elements of

Table 1

Material parameters	Unit	Quartzite	Norite
λ	MPa	1.36×10^{10}	6.36×10^{10}
μ	MPa	2.333	0.667
C_1/λ	—	−84.5	−35.0
C_2/λ	—	−5.91	−2.10
$\mathscr{R}_0$	—	1.90×10^{-2}	7.80×10^{-2}
p	—	0.15	0.15

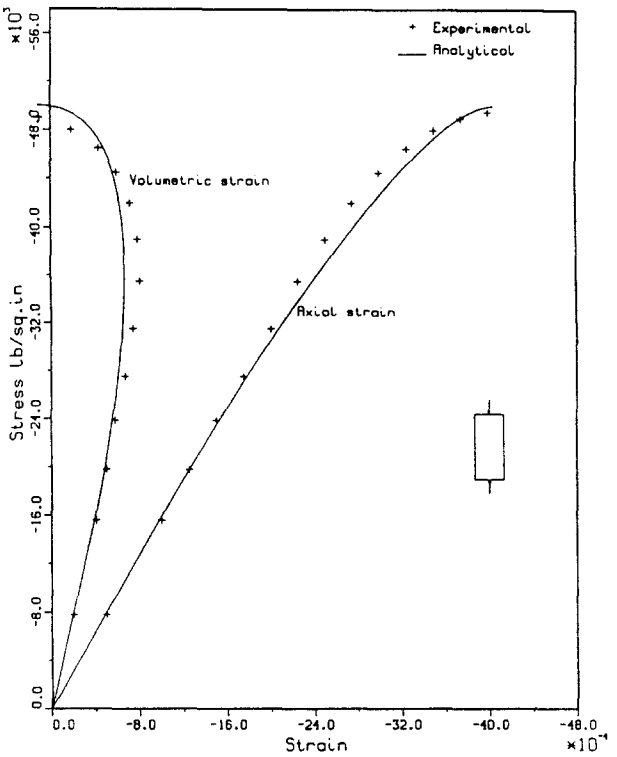

Fig. 3. Comparison of the analytical and the experimental results for norite in uniaxial compression.

the tensor **K**, while constant during unloading, are the functions of the already accumulated damage. Consequently, the unloading segment of the stress–strain curve, while straight, is not parallel to the initial segment of the initial loading.

4.3. *Results*

The computations were performed for two types of rocks, Witwatersrand quartzite and norite, and compared with experimental data (Bienawski *et al.*, 1969; Crouch, 1970) to the extent available. The hemisphere of orientation is divided into elementary surfaces with an approximately equal solid angle of $\pi/250$ and one microcrack system $(\omega, \mathbf{N})$ is assigned to each division. The material parameters of the considered materials are arranged in Table 1. The parameters C_1, C_2, and p were selected such that the calculated results present a best fit of the experimental data. The parameter $\mathscr{R}_0$ was obtained from the condition that the onset of microcracking corresponds to the stress level at which the material starts exhibiting nonlinearity.

The details of the stress–strain relationship were replicated with a high degree of accuracy for compression (Figs 3 and 4). The volumetric strain in compression reaches its maximum at approximately 85–90% of the maximum stress as observed in most of the experiments. The influence of the lateral confinement is plotted in Fig. 5. The increase of strength with lateral pressure follows the trends reported in the literature (Paterson, 1978).

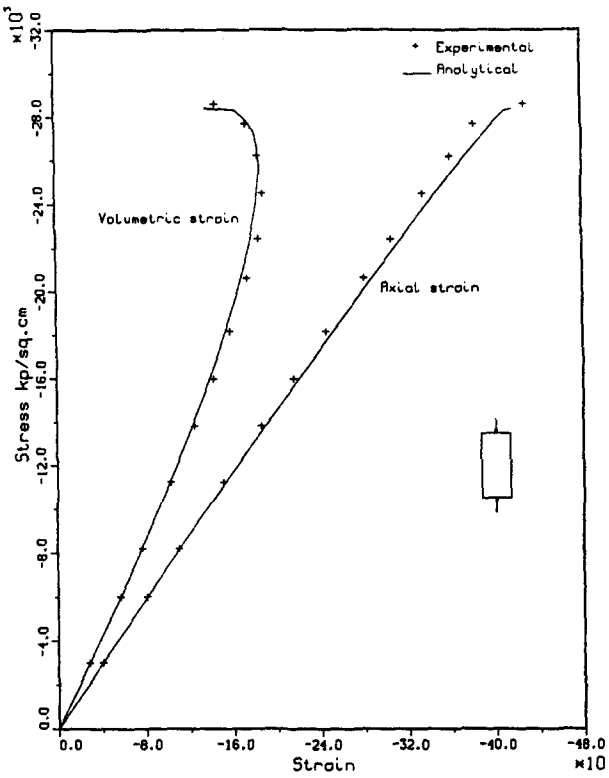

Fig. 4. Comparison of the analytical and the experimental results for Witwatersrand quartzite in uniaxial compression.

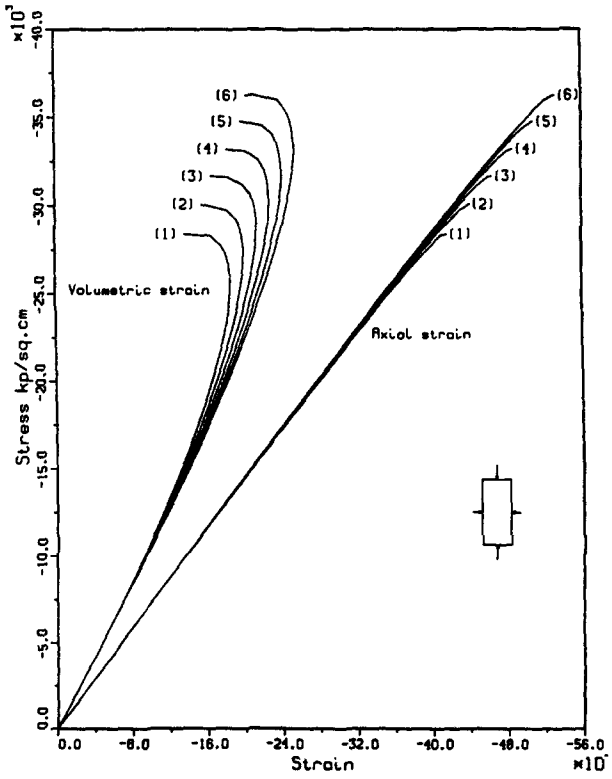

Fig. 5. Axial and volumetric stress–strain curves at low confinement pressures for quartzite. Confinement pressure: (1) unconfined; (2) 1% of C_t; (3) 2% of C_t; (4) 3% of C_t; (5) 4% of C_t; (6) 5% of C_t (where C_t is the compressive strength).

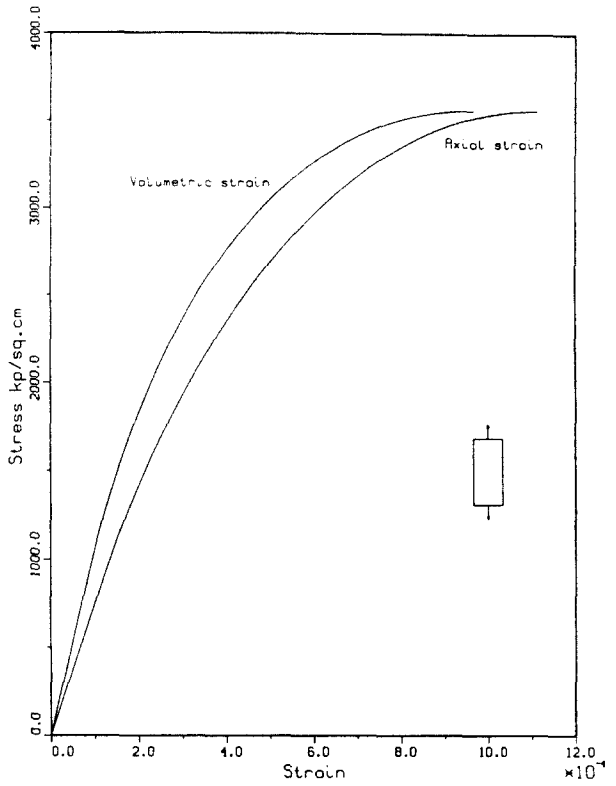

Fig. 6. Variation of axial and volumetric strain in uniaxial tension for quartzite.

The computed ratio of compressive to tensile strength is nearly ten (Fig. 6) as found in the experiments.

An especially important feature of the proposed model is its ability to predict the patterns of the microcrack distribution. The distribution of microcracks (normalized by the maximum density) is shown in Figs 7 and 8. In case of uniaxial compression the microcrack distribution has two maxima : the global corresponding to splitting and the local associated with shear, as found from experiments (Wawersik and Brace, 1971). The computed relative strength of the two maxima is within 10% of the experimental observations. The growth of microcracks with stress, in planes of various orientations, is plotted in Figs 9 and 10. Near the failure, the microcrack growth accelerates rapidly over a large range of orientations. This is in accord with the experiments (Wong, 1982), that a substantial increase in the crack density in a wide range of orientations is instrumental in forming links between the cracks which lead to faulting.

The computed biaxial tension–compression strength envelope (Fig. 11) shows basically most of the observed trends (Kupfer *et al.*, 1969; Akai and Mori, 1970; Brown, 1974). The model underestimates the biaxial compressive strength, indicating that the phenomena neglected (crack interaction, friction, etc.) may be more important than assumed. However, it has been suggested (Avram *et al.*, 1981) that the strength in biaxial compression is very sensitive to the conditions at the specimen interface with the loading device, and the use of a more sophisticated loading device lowers the strength in biaxial compression.

5. SUMMARY AND CONCLUSIONS

The proposed analytical model is developed within the framework of the continuum "damage" theory (Krajcinovic, 1985) based on the thermodynamics with internal variables. Even though the model is phenomenological in nature and relates the average values of the stress and strain, the physical insight into the phenomenon is retained to a remarkable degree through the selection of the internal variables. As a result, the model is able to replicate not only the major trends of the mechanical response but also the details related

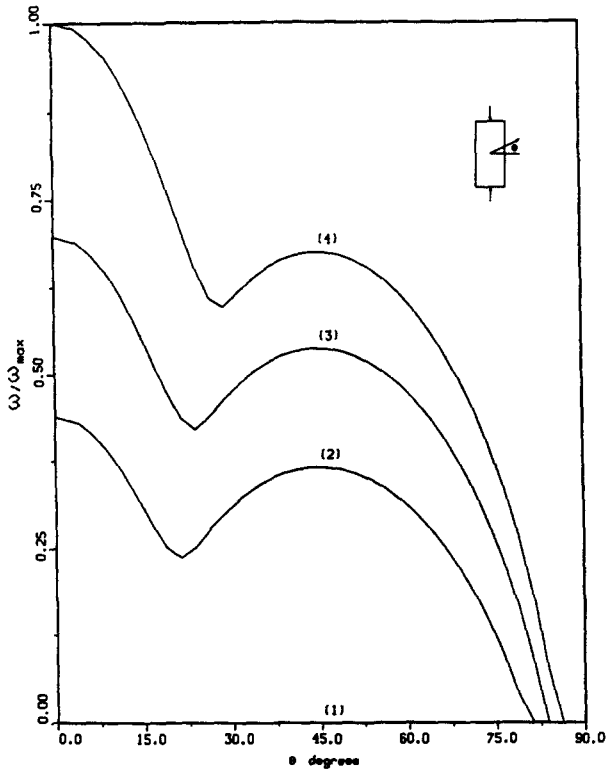

Fig. 7. Microcrack distribution at different load levels in uniaxial compression for quartzite: (1) at less than 25% of C_f; (2) at 60% of C_f; (3) at 85% of C_f; (4) at C_f (where C_f is the compressive strength).

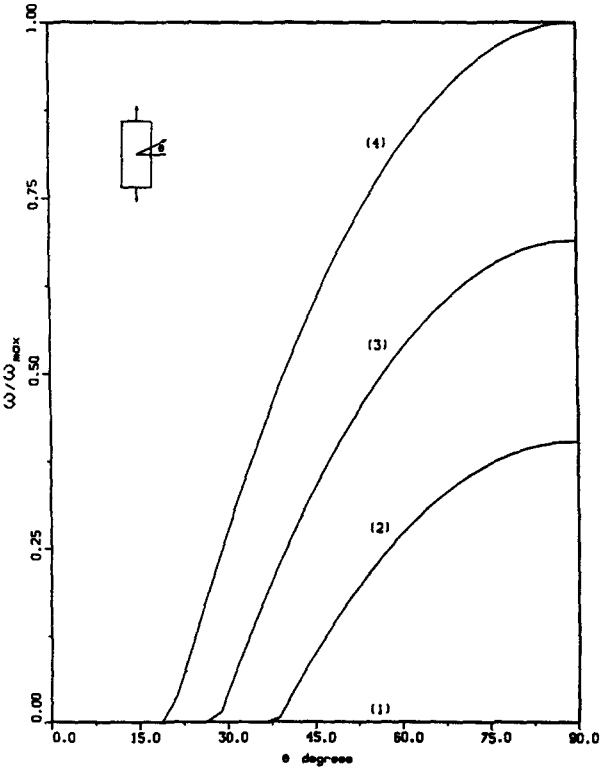

Fig. 8. Microcrack distribution at different load levels in uniaxial tension for quartzite: (1) at less than 25% of T_f; (2) at 60% of T_f; (3) at 85% of T_f; (4) at T_f (where T_f is the tensile strength).

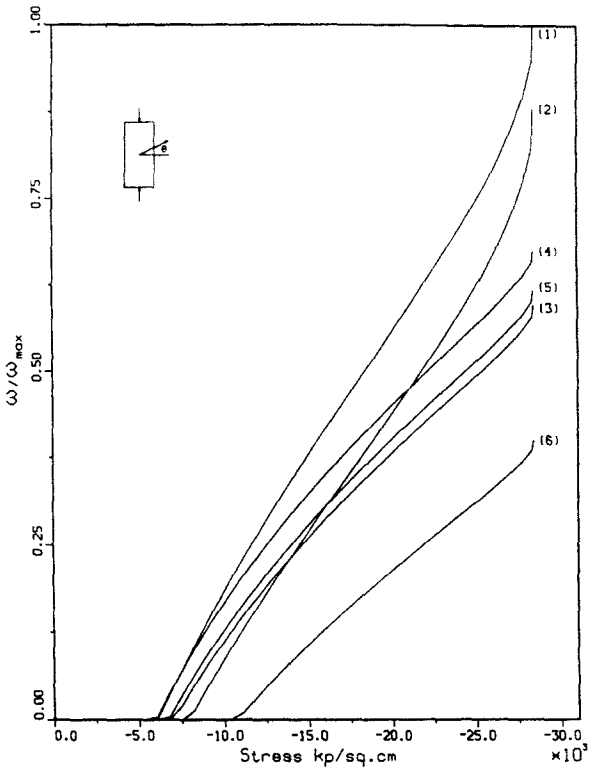

Fig. 9. Evolution of microcrack density $\omega(\theta)$ as a function of stress in uniaxial compression for quartzite: (1) $\theta = 0°$; (2) $\theta = 15°$; (3) $\theta = 30°$; (4) $\theta = 45°$; (5) $\theta = 60°$; (6) $\theta = 75°$.

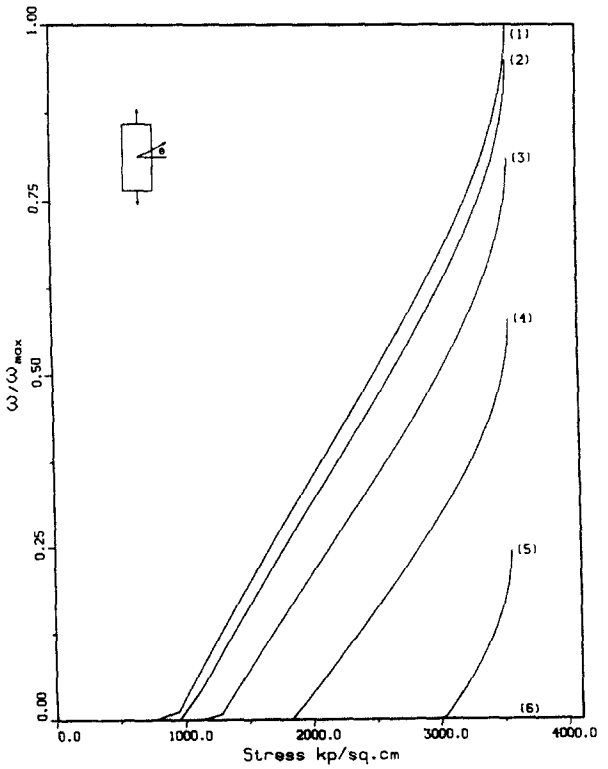

Fig. 10. Evolution of microcrack density $\omega(\theta)$ as a function of stress in uniaxial tension for quartzite: (1) $\theta = 90°$; (2) $\theta = 75°$; (3) $\theta = 60°$; (4) $\theta = 45°$; (5) $\theta = 30°$; (6) $\theta < 15°$.

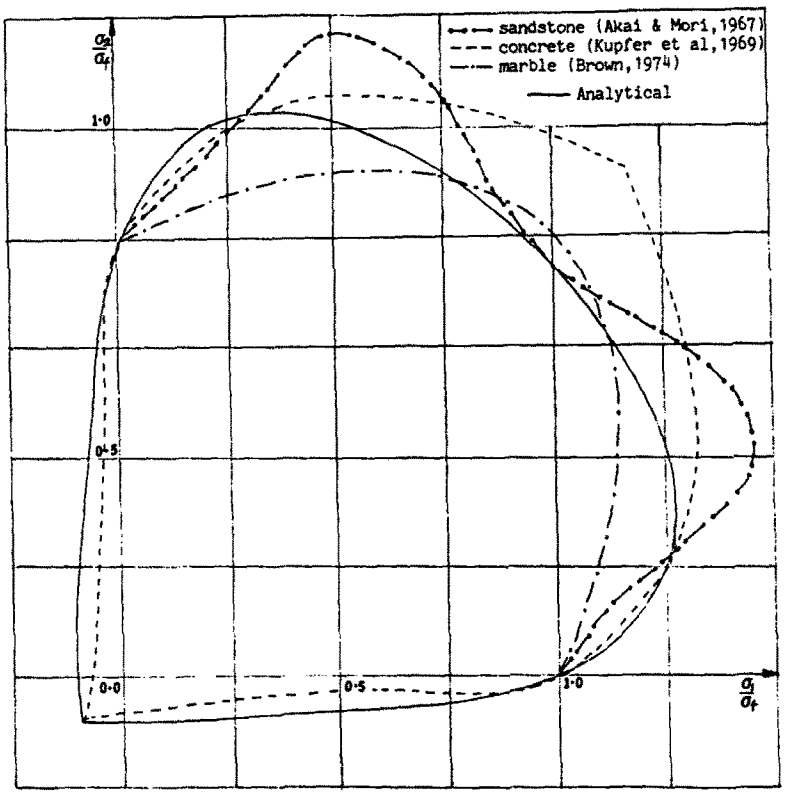

Fig. 11. Normalized failure envelope for uniaxial–biaxial loading.

to microcrack patterns, volumetric strains, etc. This, naturally, lends some credence to the expectation related to applications of this model to problems involving more complicated geometries, stress distributions, etc. The softening part of the stress–strain curve can be readily obtained by the proposed model. However, since in the post peak region microcracks coalesce to macrocracks and the heterogeneity of the deformation becomes important, the veracity of those results are questionable.

Acknowledgement—The authors gratefully acknowledge the financial support in the form of a research grant from the U.S. Department of Energy, Office of Basic Energy Sciences, Engineering Research Program to the University of Illinois at Chicago, which made this work possible.

REFERENCES

Akai, K. and Mori, H. (1970). Study on failure mechanism of a sandstone under combined stress. *Trans. Jap. Soc. Civil Engrs* **147**, 11.

Avram, C. *et al.* (1981). *Concrete Strength and Strains*. Elsevier, Amsterdam.

Bienawski, Z. T., Denkhaus, H. G. and Vogler U. W. (1969). Failure of fractured rock. *J. Rock Mech. Min. Sci. Geomech. Abstr.* **6**, 323.

Brown, E. T. (1974). Fracture of rock in uniform biaxial compression. In *Advances in Rock Mechanics, Proceedings of the Third ISRM Congress*, Vol. III, Part A.

Coleman, B. D. and Gurtin, M. E. (1967). Thermodynamics with internal state variables. *J. Chem. Phys.* **47**, 597.

Costin, L. S. (1983). Microcrack model for the deformation and failure of brittle rock. *J. Geophys. Res.* **88**, 9485.

Crouch, S. L. (1970). Experimental determination of volumetric strain in failed rock. *Int. J. Rock Mech. Min. Sci. Geomech. Abstr.* **7**, 589.

Drucker, D. C. (1959). A definition of stable inelastic material. *J. Appl. Mech.* **26**, 101.

Holcomb, D. J. (1984). Discrete memory in rock: a review. *J. Rheology* **28**, 725.

Hutchinson, J. W. (1976). Elastic plastic behaviour of polycrystalline metals and composites. *Proc. R. Soc. Lond.* **A319**, 247.

Ilankamban, R. (1985). Continuum damage theory for progressively degrading brittle solids with application to geomaterials. Ph.D. Thesis, CEMM Dept., University of Illinois at Chicago.

Krajcinovic, D. (1985). Continuous damage mechanics revisited: basic concepts and definitions. *J. Appl. Mech.* **52**, 829.

Kupfer, H., Hilsdoorf, H. F. and Rusch, H. (1969). Behaviour of concrete under biaxial stresses. *ACI J.* **66**, 656.

Nemat-Nasser, S. and Horii, H. (1982). Compression induced non-planar crack extension with application to splitting, exfoliation and rockburst. *J. Geophys. Res.* **87**, 6805.

Paterson, M. S. (1978). *Experimental Rock Deformation—The Brittle Field.* Springer, Berlin.
Spencer, A. J. M. (1971). Theory of invariants. In *Continuum Physics* (Edited by A. C. Eringen), Vol. 1. Academic Press, New York.
Sprunt, E. S. and Brace, W. F. (1974). Direct observations of microcavities in crystalline rocks. *Int. J. Rock Mech. Min. Sci. Geomech. Abstr.* **11,** 139.
Tapponnier, P. and Brace, W. F. (1976). Development of stress induced microcracks in westerly granite. *Int. J. Rock Mech. Min. Sci. Geomech. Abstr.* **13,** 103.
Wawersik, W. R. and Brace, W. F. (1971). Post failure behaviour of a granite and diabase. *Rock Mech.* **3,** 61.
Wong, T. F. (1982). Micromechanics of faulting in Westerly granite. *Int. J. Rock. Mech. Min. Sci. Geomech. Abstr.* **19,** 49.